

CrystEngComm

Accepted Manuscript



This is an *Accepted Manuscript*, which has been through the Royal Society of Chemistry peer review process and has been accepted for publication.

Accepted Manuscripts are published online shortly after acceptance, before technical editing, formatting and proof reading. Using this free service, authors can make their results available to the community, in citable form, before we publish the edited article. We will replace this *Accepted Manuscript* with the edited and formatted *Advance Article* as soon as it is available.

You can find more information about *Accepted Manuscripts* in the [Information for Authors](#).

Please note that technical editing may introduce minor changes to the text and/or graphics, which may alter content. The journal's standard [Terms & Conditions](#) and the [Ethical guidelines](#) still apply. In no event shall the Royal Society of Chemistry be held responsible for any errors or omissions in this *Accepted Manuscript* or any consequences arising from the use of any information it contains.

An unusual single crystal-to-single crystal [2+2] photocyclisation reaction of a TTF-aryl-nitrile derivative.

Cite this: DOI: 10.1039/x0xx00000x

Received 00th January 2012,
Accepted 00th January 2012

DOI: 10.1039/x0xx00000x

www.rsc.org/

John J. Hayward,^a Roger Gumbau-Brisa,^a Antonio Alberola,^b Caroline S. Clarke,^b Jeremy M. Rawson^{†b} and Melanie Pilkington^{a*}

4-([2,2'-*bi*(1,3-dithiolylidene)]-4-yl)benzotrile undergoes a [2+2] photo-cycloaddition reaction upon irradiation with polychromatic light, an unusual single-crystal-to-single-crystal transformation for a TTF derivative. In contrast, the closely related pyridynitrile derivative adopts a different packing motif and is stable to light under the same conditions.

Introduction

Within the field of solid-state organic reactions,¹ the photochemical [2+2] cycloaddition reaction between two alkenes is deserving of particular note. In solution this reaction is capable of giving rise to complex reaction mixtures, due to the differing approach vectors of the alkenes, orbital effects, and photochemical bond isomerism of the reacting functional groups. As a result, the reactions of acyclic alkenes are often only run to low conversion so as to prevent this double-bond isomerism.² In contrast, the topochemical control³ imparted by the crystalline state⁴ often results in highly diastereoselective reactions which can approach quantitative yields.⁵

Integral to this control of reactivity is the arrangement of the reactive functionality within the crystal. Solid state [2+2] reactions were first studied by Schmidt *et al.* in the 1960's who developed a set of geometrical parameters known as the "topochemical principle" to determine the outcome of a reaction.⁶ Schmidt proposed that for a cycloaddition reaction to occur, the two C=C bonds must be co-planar and no more than 4.2 Å apart.^{3,7} This arrangement occurs naturally in, for example, certain polymorphs of cinnamic acids,³ and is increasingly being engineered through the use of non-covalent interactions⁸ such as hydrogen⁹ and halogen bonding,¹⁰ coordinate bonds¹¹ and π - π arene-perfluoroarene interactions.¹²

In an analogous fashion to the solid state reactivity of alkenes, the electronic properties of tetrathiafulvalene (TTF) derivatives are highly dependent upon their solid-state topologies, with short π - π interactions between parallel stacks of their radical cation salts favourable for electrical conductivity. In this respect, TTF derivatives

have been widely employed in the field of molecular electronics as semiconductors and organic field-effect transistors,¹³ with over 10,000 papers published in this area to-date.¹⁴ Surprisingly, despite the presence of electron rich double bonds and the realization of new derivatives that promote the parallel stacking of molecules, examples of TTF donors that undergo [2+2] photo-dimerization reactions in a single crystal are extremely rare.¹⁵⁻¹⁹ The first evidence that a solid state [2+2] photo-cyclisation reaction of a TTF derivative could occur was reported in 1986 by Neilands *et al.*¹⁵ This was followed by the light induced cyclo-dimerization of *bis*(butyloxycarbonyl)TTF in 1990.¹⁶ Later, Batail and Avarvari reported the first example of a single-to-single crystal (SCSC) [2+2] photo-cyclisation²⁰ of a TTF-amidopyridine.¹⁷ In recent years, there have been three other reports of light induced solid state [2+2] cycloaddition reactions involving TTFs,^{18,19} though these do not occur *via* SCSC transformations.

As part of our research program directed towards the preparation of molecule-based magnetic and/or conducting materials we have developed synthetic strategies for the incorporation of hydrogen bonding interactions²¹ and metal binding sites²² into the organic framework of TTF donors, as well as the synthesis of the first verdazyl radical-functionalized TTF.^{22b,23} Expanding our synthetic toolbox, we recently turned our attention to prepare TTF derivatives bearing aryl nitrile substituents, since there are only a few examples of TTF donors bearing electron deficient substituents in the literature and they are versatile functional groups that can be readily converted into spin active moieties.²⁴ Furthermore, aryl nitriles, possessing a rigid structure and unhindered nitrogen atom have found applications in the field crystal engineering, with the electronegative, polarising nature of the CN group interacting strongly with softer polarisable groups such as structure-directing CN...X,²⁵ and CN...S²⁶ interactions, as well as CN...H-C^{Ar} hydrogen bonding.²⁷ In this context we report the preparation and structural study of the 4-arylnitrile substituted TTFs **1** and **3**. In both cases we observe the parallel arrangement of these donors and olefin...olefin separations of less than 4.2 Å in their crystal

structures, which prompted us to investigate the reactivity of single crystals of both compounds upon exposure to polychromatic light.

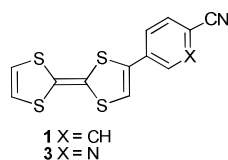


Figure 1. Molecular structures of 4-arylnitrile-TTF derivatives **1** and **3**.

Experimental section

General considerations

All experiments were performed under a nitrogen atmosphere unless stated otherwise. Dry solvents were obtained from a Puresolve PS MD-4 solvent purification system. All other chemicals were commercially available and used as received, unless otherwise stated. NMR spectra were recorded on either a Bruker Avance AV 300 or Bruker Avance AV 600 Digital NMR spectrometer with a 14.1 Tesla Ultrashield Plus magnet and chemical shifts were determined with reference to residual solvent. Samples for FT-IR were pressed as KBr pellets and their spectra were recorded using a Bomem MB-100 spectrometer. Electron Impact (EI) mass spectra were obtained using a Kratos Concept 1S High Resolution E/B mass spectrometer. Samples for elemental analysis were submitted to Atlantic Microlab, Norcross, GA. UV-Vis spectra were recorded using a ThermoSpectronic/Unicam UV-4 UV-Vis spectrometer. Melting points were obtained on a Stuart Scientific SMP 10 apparatus.

Synthesis

4-([2,2'-bi(1,3-dithiolylidene)]-4-yl)benzonitrile, **1**

TTF-4-benzonitrile **1** was synthesized as an orange solid in 62 % yield following a modification of the literature procedure (ESI-S1)²⁸. M.p.: 214 °C (dec.); ¹H NMR (600 MHz, CDCl₃, ppm): 7.66 (d, *J* = 7.95 Hz, 2H, ^{Ar}H, *ortho* to CN), 7.50 (d, *J* = 7.95 Hz, 2H, ^{Ar}H, *meta* to CN), 6.73 (s, 1H, ^{TTF}H, C-C=C-H), 6.37 (s, 2H, ^{TTF}H, H-C=C-H); ¹³C NMR (150 MHz, CDCl₃, ppm): 136.40 (^{Ar}C, *para* to CN), 134.23 (^{TTF}C, C-C=C-H), 132.66 (2 × ^{Ar}C, *ortho* to CN), 126.55 (2 × ^{Ar}C, *meta* to CN), 119.11 & 119.08 (terminal ^{TTF}C, H-C=C-H), 118.45 (C≡N), 117.80 (^{TTF}C, C-C=C-H), 113.64 (internal ^{TTF}C), 111.53 (^{Ar}C, *ipso* to CN), 107.22 (internal ^{TTF}C); FT-IR (KBr, cm⁻¹): 3059, 2224, 1575, 1535, 1405, 1312, 1285, 1176, 1092, 831, 796, 436; UV-Vis (CH₃CN, nm): λ_{max} = 290 (ε = 19100 M⁻¹ cm⁻¹), 438 (ε = 2990 M⁻¹ cm⁻¹); HR-MS (EI): calculated for [C₁₃H₇NS₄]⁺: 304.94614, found 304.94606; Elemental Analysis (%) calculated for C₁₃H₇NS₄: C 51.12, H 2.31, N 4.59; found: C 51.02, H 2.11, N 4.49.

4,4'-(2,5-di(1,3-dithiol-2-ylidene)tetrahydrocyclobuta[1,2-d:3,4-d']bis([1,3]dithiole)-3a,3b-diyl)dibenzonitrile **2**

Compound **1** was allowed to stand in the sunlight for two weeks at room temperature. Subsequent recrystallization of this material (200 mg) from MeCN afforded thin yellow plate-like single crystals of the cyclized derivative **2** (150 mg). Recovered yield 75 %; ¹H NMR (300 MHz, CDCl₃, ppm): δ_H = 7.41 (4H, d, *J* = 8.4 Hz, ^{Ar}H, *ortho* to CN), 7.20 (4H, d, *J* = 8.4 Hz, ^{Ar}H, *meta* to CN), 6.23 (4H, s, ^{TTF}H, H-C=C-H), 5.37 (2

H, s, C-C-H). ¹³C NMR (75 MHz, CDCl₃, ppm) δ_C = 144.89 (2 × ^{Ar}C, *para* to CN), 132.64 (2 × TTF-C, H₂C₂S₂C=C-S₂), 132.41 (4 × ^{Ar}C, *ortho* to CN), 128.02 (2 × TTF-C, H₂C₂S₂C=C-S₂), 127.00 (4 × ^{Ar}C, *meta* to CN), 119.40 (2 × terminal TTF-C, H-C=C-H), 119.29 (2 × terminal TTF-C, H-C=C-H), 117.90 (C≡N), 111.29 (^{Ar}C, *ipso* to CN), 62.52 (C-C-H), 57.83 (C-C-H). M.p. = 132–134 °C; UV-Vis (MeCN, nm) λ_{max} = 351 (ε = 36930 M⁻¹ cm⁻¹), 403 (ε = 15410 M⁻¹ cm⁻¹); Elemental Analysis (%) calculated for C₂₆H₁₄N₂S₈: C 51.12, H 2.31, N 4.59; found: C 51.20, H 2.54, N 4.79.

5-(2-(1,3-dithiol-2-ylidene)-1,3-dithiol-4-yl)pyridine-2-carbonitrile, **3**

A solution of TTF (1.02 g, 4.9 mmol) in dry THF (60 mL) was cooled to -83 °C and a solution of LDA (1.8 M, 3.3 mL, 6.0 mmol) was added dropwise to the solution. The reaction mixture was stirred for 1 h at -83 °C after which time a solution of ZnCl₂ (1.03 g, 7.5 mmol) in dry THF (1.5 mL) was added and the mixture stirred for an additional 1 h at -83 °C. A solution of Pd(PPh₃)₄ (0.59 g, 0.5 mmol) and 5-bromo-2-pyridylcarbonitrile (1.29 g, 7.0 mmol) in dry THF (20 mL) was then added dropwise. The reaction was kept at -83 °C for 1 h before being allowed to warm slowly to room temperature. The reaction mixture was stirred for a total of 48 h at room temperature after which time water (100 mL) and DCM (100 mL) were added. The organic phase was collected, washed with water and dried over anhydrous MgSO₄. The solvent was removed under reduced pressure and the crude product purified by column chromatography (neutral alumina, EtOAc/hexane, 1:3) to yield **3** as a dark purple powder, 1.28 g (84 % yield). M.p. = 219 °C (dec.); ¹H NMR (600 MHz, CDCl₃, ppm) δ_H = ¹H NMR (600 MHz, CDCl₃, ppm) δ_H = 8.79 (1H, d, *J* = 2.2 Hz, ^{Ar}H, *ortho* to pyridyl N), 7.76 (1H, dd, *J* = 8.3, 2.2 Hz, ^{Ar}H, *para* to pyridyl N), 7.71 (1H, d, *J* = 8.3 Hz, ^{Ar}H, *meta* to pyridyl N), 6.87 (1H, s, ^{TTF}H, C-C=C-H), 6.39 (2H, s, ^{TTF}H, H-C=C-H). ¹³C NMR (150 MHz, CDCl₃, ppm) δ_C = 147.97 (^{Ar}C, *ortho*-pyridyl), 133.56 (^{Ar}C, *para* to pyridyl N), 132.21 (^{Ar}C, *ortho* to pyridyl N, *ipso* to CN), 131.30 (TTF-C, C-C=C-H), 130.93 (^{Ar}C, *meta* to pyridyl N, *para* to CN), 128.42 (^{Ar}C, *meta* to pyridyl N, *ortho* to CN), 120.08 (^{TTF}C, C-C=C-H), 119.13 (2 × terminal ^{TTF}C, H-C=C-H), 116.99 (C≡N), 115.16 (internal ^{TTF}C), 105.98 (internal ^{TTF}C). EI-MS *m/z* = 306 [M]⁺ (78 %); FT-IR (KBr, cm⁻¹) ν = 3068, 2228, 1563, 1526, 1378, 1088, 1023, 830, 775, 658, 518, 435. UV-Vis (MeCN, nm) λ_{max} = 304 (ε = 28300 M⁻¹ cm⁻¹), 480 (ε = 3870 M⁻¹ cm⁻¹); Elemental Analysis (%) calculated for C₁₂H₆N₂S₄: C 47.03, H 1.97, N 9.14, S 41.85; found: C 46.81, H 1.86, N 9.16, S 41.16.

Computational studies

DFT calculations were undertaken on **1** and **3**. Initial geometry optimisations were undertaken using the Pople²⁹ 6-31G** basis set and B3LYP³⁰ functional within Jaguar.³¹ Subsequent single-point energy calculations were performed on the optimised structures using the larger triple zeta 6-311G-3DF-3PD basis set.³²

X-ray structure determination

Single crystals of **1** and **2** were mounted on a glass fibre in fluoropolymer and examined on a Nonius Kappa CCD area detector equipped with an Oxford Cryoflex low temperature device. Data were measured at 180(2) K using Mo-Kα radiation (λ = 0.71073 Å) using the Nonius COLLECT.³³ Data reduction and cell refinement implemented DENZO and Scalepack,³⁴ and an absorption correction applied using symmetry-related equivalents (Sortav).³⁵ A crystal of **3** was mounted

in a cryoloop with paratone oil and examined on a Bruker APEX-II CCD diffractometer equipped with a CCD area detector and an Oxford Cryoflex low temperature device. Data were measured at 120(2) K with Mo-K α radiation ($\lambda = 0.71073 \text{ \AA}$) using the APEX-II software.³⁶ Cell refinement and data-reduction were carried out by SAINT.³⁶ An absorption correction was performed by the multi-scan method implemented in SADABS.³⁶ The structures of **1** and **2** were solved using SIR-92 and the structure of **3** solved by direct methods (SHELXS-97).³⁷ All three structures were refined using SHELXL-97³⁷ in the Bruker SHELXTL suite.³⁶ The structure of **1** exhibited substantial disorder which was modelled over two sites, comprising one dimer (80 %) and two monomers (20 %). All non-H atoms in the major component of the disorder were refined anisotropically as well as the S atoms in the minor component. One of the C₃S₂ fragments of the minor component of disorder appeared coincident with the major component and these atoms were refined anisotropically with both their positions and U(ij) parameters constrained to be equivalent to the major component of the disorder. The remaining C and N atoms of the minor component were refined isotropically with their U_{iso} restrained to be equivalent to the corresponding atoms in the main component of disorder. H atoms were added at calculated positions and refined with a riding model. In the case of **3**, anisotropic refinement of all non-H atoms proceeded smoothly but stalled at R₁ ~ 17 % with a large number of disagreeable reflections with F_o > F_c indicative of twinning. The data were examined with TwinRotMat within PLATON.³⁸ and a minor twin identified which was included in the latter stages of refinement (TWIN/BASF). Hydrogen atoms were added at calculated positions and refined with a riding model. Crystallographic parameters for **1** – **3** are summarized in Table 1. Selected bond lengths and angles for **1**, **2** and **3** are provided in the ESI (S-2).[†] The structures have been allocated the following CCDC deposition numbers CCD 986761 – 986763.

Table 1. Crystallographic data for **1**, **2** and **3**.

Compound reference	1	2	3
Chemical formula	C ₁₃ H ₇ NS ₄	C ₂₆ H ₁₄ N ₂ S ₈	C ₁₂ H ₆ N ₂ S ₄
Formula Mass	305.44	610.88	306.43
Crystal system	Monoclinic	Monoclinic	Monoclinic
<i>a</i> /Å	11.274(2)	11.119(2)	3.9337(4)
<i>b</i> /Å	8.2761(17)	8.3345(17)	11.3951(9)
<i>c</i> /Å	27.958(6)	28.069(6)	27.644(2)
<i>a</i> /°	90	90	90
<i>β</i> /°	95.47(3)	95.85(3)	91.393(5)
<i>γ</i> /°	90	90	90
Unit cell volume/Å ³	2596.74	2587.64	1238.77
Temperature/K	180(2)	180(2)	150
Space group	<i>P</i> 2 ₁ / <i>n</i>	<i>P</i> 2 ₁ / <i>n</i>	<i>P</i> 2 ₁ / <i>c</i>
<i>Z</i>	8	4	4
No. of reflections measured	11691	9111	17919
No. of independent reflections	3658	2794	1613
<i>R</i> _{int}	0.060	0.0459	0.0627
Final <i>R</i> ₁ values (<i>I</i> > 2σ(<i>I</i>))	0.0365	0.049	0.0849
Final <i>wR</i> (<i>F</i> ²) values (<i>I</i> > 2σ(<i>I</i>))	0.0745	0.0789	0.2579
Final <i>R</i> ₁ values (all data)	0.0491	0.0365	0.0959
Final <i>wR</i> (<i>F</i> ²) values (all data)	0.0789	0.0745	0.2704

Results and discussion

The TTF-benzonitrile donor **1** was prepared as an orange solid in 62 % yield via a modification of the literature method.²⁸ Unfortunately this methodology afforded poor yields of **3** so an alternative strategy involving the Negishi coupling of a TTF-ZnCl intermediate with 5-bromo-2-pyridylcarbonitrile was employed to afford **3** as a red/orange solid in 80 % yield. Both compounds were characterized by NMR, UV-Vis and IR spectroscopy, as well as EI mass spectrometry, cyclic voltammetry and CHN elemental analysis. The FT-IR spectra of **1** and **3** show ν_{C≡N} vibrations at 2224 and 2228 cm⁻¹ respectively. The UV-Vis spectra of both compounds in acetonitrile show two distinct absorption bands; the first at λ_{max} = 290 nm for **1** and 304 nm for **3**, assigned to the overlap of the transitions within the TTF and aryl nitrile moieties^{21b} and a second, red-shifted intramolecular transfer (ICT) band at λ_{max} = 438 nm for **1** and 510 nm for **3** highlighting the electronic communication between the donor TTF and acceptor Aryl-CN groups. Cyclic voltammetry measurements of acetonitrile solutions of **1** and **3** show two reversible redox waves corresponding to the oxidation of the TTF core affording the radical cation and dication respectively (Table 2).

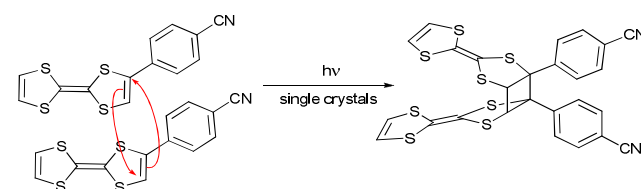
Table 2. CV oxidation potentials for TTF and derivatives **1** and **3**.^a

	E ₁ ^{1/2}	E ₁ ^{1/2}
TTF	0.37 V	0.76 V
1 ^b	0.45 V	0.82 V
3	0.48 V	0.85 V

^a0.1 M in MeCN, 0.1 mM nBu₄NPF₆; ^b Previously reported values: E₁^{1/2} = 0.47 V, E₁^{1/2} = 0.87 V in PhCN.¹⁷

These data are in agreement with the DFT studies (ESI-S3)[†] which reveal the HOMO of **1** and **3** to be of TTF character. For both compounds, the redox potentials are shifted to higher values in relation to unsubstituted TTF due to the extended delocalisation of electron density over the aromatic ring coupled with the presence of an electron-withdrawing nitrile substituent.

Single crystals of **1** were grown by slow evaporation of an acetonitrile solution. After exposure to light the crystals changed from red/orange to yellow, consistent with a loss of conjugation due to the light induced [2+2] photo-dimerization process shown in Scheme 1.¹⁷



Scheme 1. Photo-dimerisation of **1** to yield cyclized dimer **2**.

Initial evidence for this cyclisation came from the ¹H NMR spectrum that revealed the co-existence of a signal at 6.23 ppm (s, ^{sp}²C-H) assigned to the alkene proton adjacent to the benzonitrile substituent in the TTF monomer **1** and an additional signal at 5.37 ppm (s, ^{sp}³C-H), assigned to the two protons of the cyclobutane ring of the cyclized dimer **2**. Fortunately, single crystals of this material remained intact during a partial cyclisation process which facilitated a

correlation between the crystal packing of TTF-benzonitrile molecules in the monomer **1** and their dimerised cycloaddition adduct **2**.

Compound **1** crystallizes in the monoclinic spacegroup $P2_1/n$ with four independent molecules in the asymmetric unit. The molecular structure confirms that in the single crystal, molecules of **1** have undergone an incomplete photo-induced cyclisation reaction and that the single crystal comprises a disordered mixture of **1** and its [2+2] cycloaddition adduct **2**. In this respect, the asymmetric unit is comprised of a superposition of two independent molecules of **1** (20 %) and one independent molecule of the dimer **2** (80 %) (Figure 2),

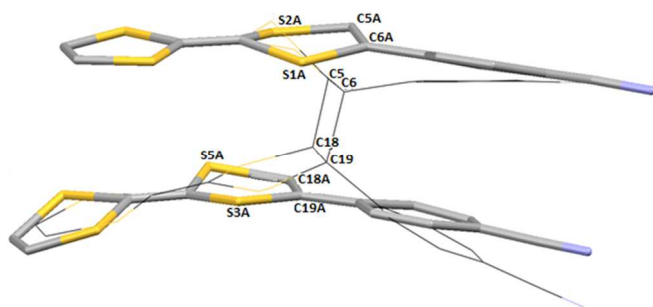


Figure 2. Molecular structure of the partially irradiated crystal. Molecules of **1** are shown as capped sticks and molecules of the cycloaddition adduct **2** are shown as a wireframe; H-atoms are omitted for clarity.

This is the first example of a SCSC [2+2] photo-cyclisation reaction where the structure determination reveals a mixture of both uncyclized **1** and cyclized **2** TTF derivatives. Due to the inherent reactivity of **1**, with respect to this [2+2] cycloaddition, it has not been possible to determine the crystal structure of pure, uncyclized **1** to-date. Nevertheless, an examination of the uncyclized component reveals that the two crystallographically independent molecules of **1** are organized into dimers. Within this dimeric unit, one TTF molecule is close to planarity, whereas the second is bowed due to small bends of 14° and 16° about its $S(3A)\cdots S(5A)$ and $S(7A)\cdots S(8A)$ vectors, respectively (Figure 3).^{19b} With over 3,000 crystal structures of TTF derivatives reported in the literature, there are multiple examples of both planar and bowed geometries.³⁹

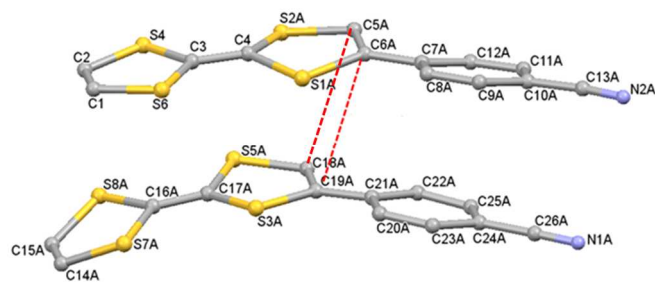


Figure 3. The crystal structure of **1** with atom labelling scheme illustrating the relative displacement of the two crystallographically independent molecules of **1** which form the dimer; H atoms are omitted for clarity. The intermolecular C...C contacts between the pairs of sp^2C atoms involved in the [2+2] cycloaddition are highlighted as red dashed lines. $C5(A)\cdots C18(A) = 3.73(3)$ Å and $C8(A)\cdots C19(A) = 3.70(5)$ Å.

These dimers are organized in a co-facial, head-to-head topology with the two benzonitrile substituents arranged mutually *cis*. The two

TTF molecules within the dimer unit are close to co-parallel with an angle of just 9° between their mean planes. Notably the intermolecular distances between the C=C units involved in the [2+2] cycloaddition reaction are just $3.70(5)$ Å and $3.73(5)$ Å, well within the 4.2 Å distance necessary for cyclisation defined by Schmidt. The two aryl substituents are also near co-planar (with an angle of 5.24° between their best planes) and are separated by $3.72(5)$ Å, consistent with π - π interactions (Figure 3). These pairs of uncyclised TTF derivatives pack in a double herringbone arrangement along the *c*-axis of the unit cell, a common packing motif for TTF derivatives (Figure 4).¹⁹ The shortest S...S contacts within the dimers comprise $S(2A)\cdots S(5A) = 3.61(5)$ Å and $S(1A)\cdots S(3A)$ at $3.66(5)$ Å. Between dimers there are additional lateral S...S contacts close to the TTF plane comprising $S(4A)\cdots S(7A)$ $3.44(7)$ Å, $S(2A)\cdots(7A)$ $3.82(5)$ Å and $S(2A)\cdots S(3A)$ $3.58(7)$ Å, (Figure 5).

The nitrile groups of both low-partial-occupancy monomer molecules show minor $CN\cdots H-C$ contacts with C-H hydrogen atoms from neighbouring C_3S_2 rings. The $N(2A)$ atom has two contacts with $C(2A)-H(2A)\cdots N(2A)^\ddagger = 2.50$ Å and $C(14A)-H(14A)\cdots N(2A)^\ddagger = 2.14$ Å, whilst $N(1A)$ forms a single short contact $C(15A)-H(15A)\cdots N(1A)^\ddagger = 2.10$ Å (where the ‡ and ‡ symbols indicate equivalent positions $(1/2+x, 3/2-y, -1/2+z)$ and $(1/2+x, 1/2-y, -1/2+z)$ respectively).

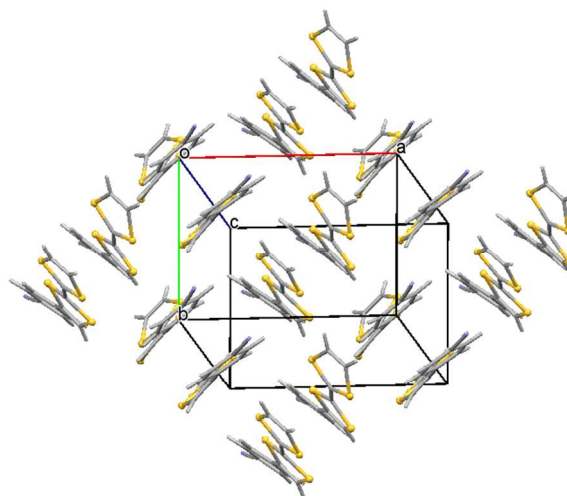


Figure 4. Crystal packing of **1** in the *ab*-plane showing the double herringbone motif.

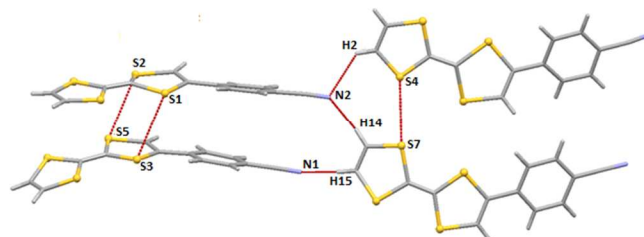


Figure 5. Intermolecular interactions in the crystal packing of **1** showing selected S...S contacts and hydrogen-bonding interactions as red dashed lines.

An overlay of the two components of the disorder within **1** clearly reveals the changes undertaken during the [2+2] photodimerisation

process (Figure 2). The loss of the π -electron system of the reacting double bonds of the TTF core accompanying the formation of the cyclobutane ring is evidenced by comparing the lengths of the C=C bond distances in the C_3S_2 rings of **1** (C(5A)–C(6A) = 1.36(5) Å and C(18A)–C(19A) = 1.33(6) Å) with their counterparts in **2** that are longer and both equivalent at 1.56(1) Å (Figure 6). This is matched with a change in C...C distances from non-bonding 3.70(5) and 3.73(5) Å in **1** which, whilst a little longer than conventional C–C bonds, are consistent with conventional C–C single bonds (1.58(1) and 1.65(1) Å). The cyclisation also leads to a change in geometry at the four reactive carbon centres as they move from trigonal planar towards tetrahedral. This is also accompanied by a significant bending about the S...S vector in the C_3S_2 ring of the first molecule, from 2.13° for S(1A)···S(2A) in monomer **1**, to 44.31° for S(1)···S(2) in cycloadduct **2**; where the bending is defined as the dihedral angle between the mean planes through S(1A)S(2A)C(4A) and C(5A)C(6A)S(1A)S(2A) for **1** and S(1)S(2)C(4) and C(5)C(6)S(1)S(2) for **2**. Notably, the first molecule of the dimer remains virtually unaffected in terms of the position of its uncyclised C_3S_2 ring (Figure 2, top), but the cyclisation of the second molecule in the asymmetric unit is accommodated by a significant displacement in the atomic positions of its second uncyclised C_3S_2 ring (for example the S atoms in the TTF ring are displaced by between 0.46(2) and 0.73(1) Å). As expected, the changes in geometry accompanying the cyclisation reaction also have a marked impact on the orientation of the two benzonitrile substituents that are almost co-planar with their attached C_3S_2 rings in monomer **1**, but are twisted by angles of 33.82° and 41.27° away from the best planes of their C_3S_2 rings in the cyclized dimer **2**. In turn, the change in the orientation of the benzonitrile substituents after cyclisation has a significant effect on both the type and range of the intermolecular interactions in the crystal packing of **2**.

To study the nature of these molecular interactions in more detail, the partially cyclized material was recrystallized from acetonitrile affording single crystals of the fully cyclized adduct that was characterized by X-ray crystallography. Taking into account small changes to the unit cell parameters, presumably arising from release of strain in **1** achieved upon recrystallization, crystals of pure **2** were found to be isomorphous with the initial structure. The molecular structure of the fully cyclized adduct is shown in Figure 6.

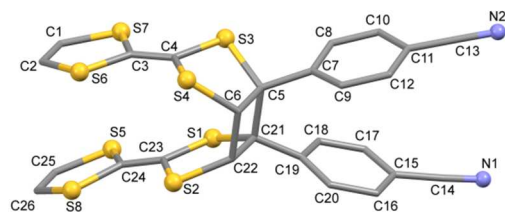


Figure 6. Molecular structure of **2**; Cyclobutane adduct: C(5)–C(6) 1.562(5), C(21)–C(22) 1.559(5), C(6)–C(22) 1.558(5) and C(5)–C(21) 1.638(5) Å; C(5)C(6)C(22) 91.6(3), C(6)C(5)C(21) 88.2(3), C(5)C(21)C(22) 88.8(2), C(6)C(22)C(21) 91.3(3)°.

The absence of disorder afforded more accurate determination of the geometry and, for example of the C–C bonds of the cyclobutane ring are C(5)–C(21) = 1.638(5) Å and C(6)–C(22) = 1.558(5) Å with the C(5)–C(6) and C(21)–C(22) bonds lengthened by 0.20 Å and 0.24 Å,

when compared to the double bonds of the undimerised monomers. The bottom TTF molecule of the dimer is close to planar, but in the top molecule, the S(3) and S(4) atoms of the hinge are displaced out of the best plane of the TTF rings by 0.487 and 0.466 Å respectively (Figure 6). Furthermore, after cyclisation the co-planarity of the TTF cores in the dimer is lost with their best planes now tilted by an angle of 19.41°. The shortest intramolecular S...S interactions within a dimer are between 3.269(2) and 3.764(2) Å.

The cyclized TTF units in **2** crystallize in a herringbone arrangement with lateral S...S contacts in the range of 3.552(2) to 3.942(2) Å (Figure 7). After cyclisation, the benzonitrile substituents are displaced from a *cis* co-planar arrangement and are tilted by an angle of 22.19° which results in the loss of the π - π interactions between their two aromatic rings. Once again the CN unit adopts a position so as to optimize C≡N...H–C contacts. Whereas in **1** both cyano groups were involved in C≡N...H–C hydrogen bonds to TTF (Figure 5), in the dimeric form **2**, only one of the original C≡N...H–C contacts to a TTF C–H bond is retained. The other two bifurcated short interactions are replaced by longer $^{Ar}C-H\cdots N$ contacts (Figure 7b).

To shed more light on the geometrical requirements for this [2+2] reaction in the solid state, we investigated the crystal structure of the closely related pyridyl analogue **3** in which CH is replaced by isolobal N. Single crystals of the TTF-pyridyl nitrile derivative were once again grown *via* the slow evaporation of an acetonitrile solution. In contrast to **1**, there was no evidence for a topochemical reaction and notably when **3** was irradiated under identical conditions to **1** there was no change in crystal colour or any spectroscopic evidence to indicate that any cyclisation had occurred even after several weeks.

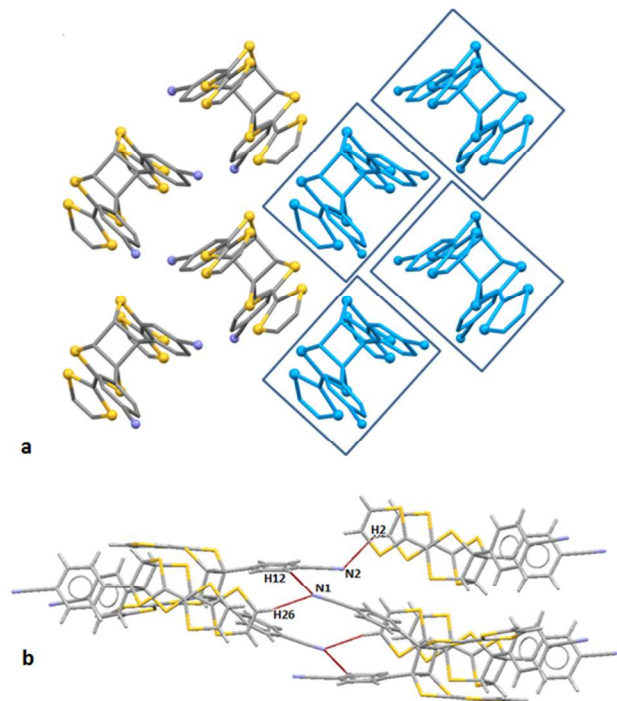


Figure 7. a) Crystal packing of **2** viewed parallel to the crystallographic *c*-axis showing the herringbone motif; b) Hydrogen bonding motif (red dashed lines) in the crystal packing of **2**. C(26)–H...N(1) = 2.550(5) Å; C(12)–H...N(1) = 2.580(4) Å and C(2)–H...N(2) = 2.591(5) Å.

Compound **3** also crystallizes in a monoclinic primitive cell but with a halving of one axis (Table 1). As a consequence the $P2_1/c$ setting contains just one molecule in the asymmetric unit (Figure 8). Molecules of **3** are co-planar and stack along the a -axis forming herringbone sheets in the ab -plane (Figure 9b). Within each stack the molecules pack in a head-to-head manner and are related by translation along the crystallographic a -axis. As a consequence the intra-stack S...S distances are equivalent at 3.934(3) Å. The intra-stack C...C separation between C=C units is also the same (3.93(1) Å) and whilst this is substantially longer than for **1**, it is well within the favourable 4.2 Å Schmidt limit for a [2+2] topochemical cycloaddition reaction (*vide infra*).³ Between the regularly spaced π -stacks there is a pair of symmetry-equivalent S...S contacts which link molecules parallel to b (S(3)...S(4) at 3.599(3) Å). Whilst the cyano group in both **1** and **2** exhibited a propensity to adopt CN...H-C contacts, in **3** these are replaced by CN...S contacts (N(2)...S(2) at 3.049(9) Å).

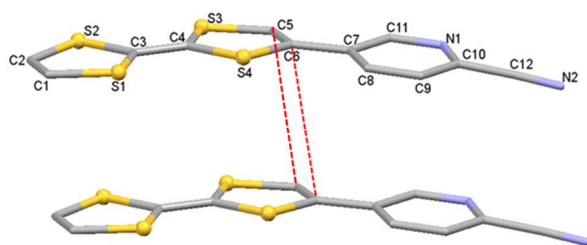


Figure 8. Molecular structure of **3** highlighting the distance of 3.93(1) Å between the outer carbon atoms of the C=C group bearing the pyridyl nitrile functionality as red dashed lines, which incidentally also corresponds to the length of the a -axis of the unit cell.

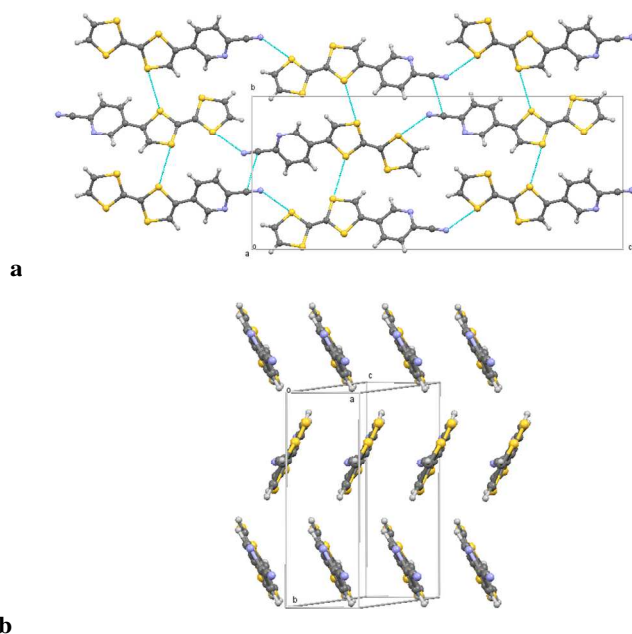


Figure 9. Crystal Packing of **3**. a) view in the bc -plane showing the S...S and CN...S contacts between π -stacks; b) view of the herringbone motif of **3**.

Interestingly, the dimensions of the unit cell of **3** ($a = 3.9337(4)$ Å; $b = 11.3951(9)$ Å; $c = 27.644(2)$ Å) are very similar to the unit cell for the

recently reported TTF-derivative bearing a carboxylic acid substituent **4**.^{19b} This compound is reported to undergo a very slow light induced [2+2] cycloaddition reaction that is attributed to strong hydrogen bonding interactions that diminish the softness of the lattice. In sharp contrast, there are no significant hydrogen bonding interactions in the crystal packing of **3**. As described above these comprise lateral S...S and CN...S interactions. A comparison of the crystal packing of compounds **3** and **4** is shown in Figure 10. Both structures adopt a regular π -stack parallel to the crystallographic a -axis. However in compound **4** the carboxylic acid dimer motif drives a head-to-head arrangement of molecules,^{19b} whereas in **3** the CN...S contacts generate head-to-tail alignment of molecules. With similar C...C distances between alkene rings along the stacking direction, it seems unlikely that the hydrogen bonding interactions in **4** are solely responsible for the slow rate of cyclisation, particularly given that **3** does not appear to cyclize at all. Comparing the separation between the two molecules in the solid state for **3** and **4** (Table 3), it is apparent that the distances between the reactive ethylene groups are slightly longer in **3** which might be a contributing factor to its lack of reactivity.

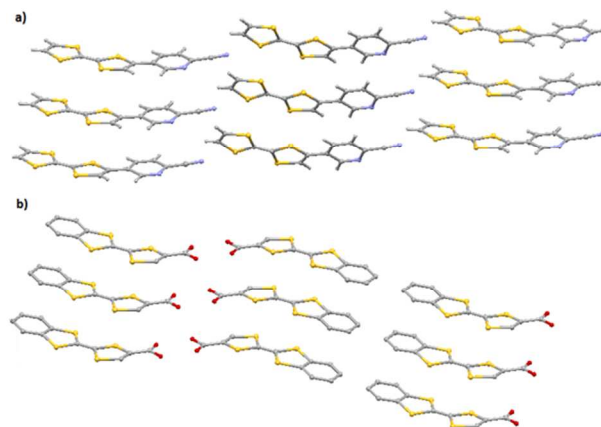


Figure 10. Crystal packing diagrams for **3** and **4**^{19b}, showing the different arrangements of the TTF donors in alternate stacks.

Given the large number of TTF derivatives reported in the literature and the common π - π stacked motif, the paucity of examples of [2+2] cycloadditions was at first surprising. In order to probe the reactivity differences between compounds **1** and **3**, DFT calculations were undertaken on geometry-optimized structures. The conventional [2+2] cyclisation is thermally forbidden but photochemically allowed due to the symmetry mismatch between the HOMO and LUMO of the alkene groups. In a light-induced [2+2] cycloaddition reaction, the cyclisation is non-concerted involving a HOMO-LUMO interaction. Moreover, the cycloaddition reaction depends upon the spatial overlap and energy match of the frontier orbitals. Thus Schmidt's cut-off distance of 4.2 Å for solid-state [2+2] reactions is a necessary pre-requisite, but the energies of the frontier orbitals must also be considered. The frontier orbitals determined at the B₃LYP 6-31G*+ level reveal that the HOMO is located on the TTF donor and the LUMO is delocalized on both the aryl nitrile derivative and the ethylene carbon atoms of the substituted C₃S₂ ring (ESI, S-3). The coefficients on the frontier orbitals are therefore consistent with

the substituted ends of the TTF molecules participating in the cycloaddition reaction with the substituted C centre most likely involved in the initial bond forming process.

The HOMO and LUMO energies for unsubstituted TTF were calculated to be -445.4 kJ/mol and -118.4 kJ/mol respectively yielding a HOMO-LUMO energy gap of 327.0 kJ/mol. Calculations upon the substituted systems **1** and **3** reveal that these energies have been substantially reduced; in each case the electron-withdrawing nitrile group serves to lower the energies of both the LUMOs (-211.7 kJ/mol for **1** and -238.3 kJ/mol for **3**) and the HOMOs (-466.7 kJ/mol for **1** and 479.9 kJ/mol for **3**), despite the increased conjugation of the system. The presence of the pyridyl nitrogen atom in **3** further lowers the energies of its frontier orbitals; the energy of the HOMO is moderately perturbed but the LUMO is more significantly lowered. These factors result in a decrease in the HOMO-LUMO energy gap from 255.0 kJ/mol for **1** to 241.6 kJ/mol for **3**, both of which can be considered within the energy range for visible light.² Given these results we can conclude that the differences in photoreactivity between **1** and **3** are not due to differences in the localization of electrons in the orbitals. Notably the structure of **4** offers a similar spatial overlap to **3** but, whilst reaction does occur in this case, the reaction appears slow. As a consequence for these TTF derivatives both the HOMO-LUMO energy gap and spatial overlap seem significant.

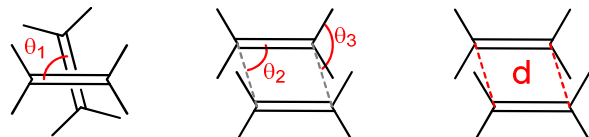
In order to shed more light on the geometrical criteria that favour solid state [2+2] photocyclization reactions in TTF derivatives we applied the geometrical criteria first introduced by Schmidt.^{3,4,40} The relative orientations of the alkenes are described in terms of (i) the distances between the two carbon atoms of the reactive double bonds;⁴⁰ (ii) θ_1 , a measure of the parallel alignment of the double bonds; (iii) θ_2 , the acute angle of the parallelogram formed by the four carbon atoms involved in the [2+2] cycloaddition and reflects the longitudinal slippage of the two π -bonds parallel to the C=C bond vector; and (iv) θ_3 , the angle between the least square plane through the four reacting C atoms and the plane passing through the C_2S_2 component of each C_3S_2 ring involved in the cycloaddition reaction.^{4,40} This reflects the latitudinal slippage of the two π -bonds. The ideal values for θ_1, θ_2 and θ_3 are $0, 90$ and 90° respectively, since Schmidt proposed that these values lead to ideal π -overlap between the reactive alkene groups in a range of alkenes that undergo light-induced cyclisation reactions.⁴⁰ The values of d, θ_1, θ_2 and θ_3 for compounds **1** and **3** as well as five reported TTF monomers (**4** – **8**, Figure 11) capable of undergoing light induced [2+2] cycloaddition reactions in the solid state are summarized in Table 3.

Only compounds in which the C_3S_2 rings of the reacting TTF derivatives are oriented appropriately in the solid state to participate in the [2+2] cyclisation reactions are compared. It should be noted that all compounds except **7**, afford *cis*-dimerised products, which is most likely due to the propensity of TTF donors to stack in a co-facial arrangement stabilized by π - π interactions. Furthermore, only compounds **1** and **7** undergo SCSC [2+2] photo-induced cyclisation reactions (Table 3, underlined).

From these data it is apparent that all seven compounds are comprised of TTF donors bearing electron withdrawing substituents which presumably favour lower HOMO-LUMO gaps and have a set of reactive alkene carbons within the 4.2 Å limit for favourable

cyclisation. Furthermore, all of the alkene groups in these compounds are organized in a co-parallel manner with the largest deviations being found in the molecular structures of the CF_3 -substituted derivatives **5** and **6**, both of which undergo cyclisation reactions in the solid state. This suggests that there is some tolerance with regards to the deviation of these reactive groups from co-planarity in TTF systems. The cyclisation of **1** and **7** gives cyclobutanes that are essentially planar; however, there is a noticeable puckering in the ring

Table 3. Schmidt parameters used to evaluate the geometrical criteria for the photo-dimerization of TTF-derivatives to occur in the solid-state.⁴⁰



	d [Å]	θ_1 [°]	θ_2 [°]	θ_3 [°]	Cyclize yes/no	^c Bu bend [°]	Ref
1	<u>3.70</u> <u>3.69</u>	<u>1.3</u>	<u>90.7</u> <u>90.3</u>	<u>63.9</u> <u>72.0</u>	yes	<u>0.61</u>	<i>this study</i>
3	3.93	0	115.4	88.6	no	-	<i>this study</i>
4	3.85	0	114.0	86.5	yes (v.slow)	5.71	^{19b}
5	3.75 4.05	9.2 9.3	93.6 95.1	69.4 74.8	yes	11.41	¹⁸
6	3.79 3.76	3.5 3.3	90.3 91.0	71.0 75.8	yes	13.43	¹⁸
7	<u>3.80</u>	<u>0</u>	<u>108.4</u>	<u>75.7</u>	yes	<u>0</u>	¹⁷
8	3.95	0.19	99.6 99.1	64.3 61.8	yes	No data	¹⁶

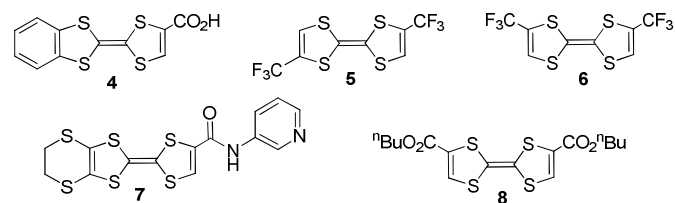


Figure 11. Five reported TTF monomers for which single crystal data is available that undergo a [2+2] photo-cycloaddition reactions in the solid state.¹⁶⁻¹⁹

geometry of the products of **4**, **5** and **6**, (^cBu bend, Table 3). Reviewing the data in the Table 3 it is clear that compound **1** has the shortest C=C to C=C distances and that the two double bonds are almost co-planar with θ_2 angles very close to 90° . Although their θ_3 values deviate substantially from 90° , they are within the $64 - 89^\circ$ range found for the other six compounds. The deviation of these angles from 90° is most likely a consequence of the diverse range of substituents directly attached to the cyclobutane ring. We can therefore conclude that this compound fulfils the entire geometrical criterion for a photo-induced cyclisation in the solid state which is consistent with our experimental observations. Comparing compound **3** which does not cyclize and compound **4** which cyclizes, albeit very slowly, it becomes obvious that a significant parameter in determining whether or not a cyclisation reaction is favourable for this family of

systems is the size of the θ_2 angle which reflects longitudinal slippage. This angle reflects how close in geometry the functionality is to the 90° angle favourable for the formation of the cyclobutane ring during the cyclisation process. The large θ_2 angles in **3** and **4** reflect large longitudinal slippage which will reduce orbital overlap and require more translational movement within the crystal lattice in order for the photo-dimerization reaction to take place. In addition, for compound **3**, the slightly longer C=C to C=C lengths also disfavour the cyclisation, whereas for **4**, the slightly shorter distances enable the molecules to undergo the required molecular motions, but it is likely that the process takes time since large geometrical changes have to be accommodated by the crystalline lattice. The large geometrical changes in **4** are also consistent with the crystal breaking, disfavoured a SCSC photocyclisation process which is consistent with the experimental observations.^{19b}

Conclusions

The propensity of TTF donors to adopt either regular π -stacks or π - π dimers with S...S distances of less than 4.2 Å makes this family of systems attractive for the study of photoinduced [2+2] cycloaddition reactions in the solid state. Indeed, a search of the Cambridge Structural Database for TTFs with intermolecular C=C to C=C bond distances of 3.6 ± 0.6 Å revealed more than 1500 hits with mean C=C bond distances of 3.9 Å, all within Schmidt's cut-off distance of 4.2 Å for favourable [2+2] cycloadditions. Despite these findings only a handful of TTF derivatives undergo such solid state reactions. We believe this is attributable to an additional non-geometric requirement for cyclisation, i.e. a small HOMO-LUMO gap. The presence of an electron-withdrawing group in addition to the required geometry appears critical to sufficiently reduce the HOMO-LUMO gap and promote this solid state transformation. TTF derivatives with electron-withdrawing substituents are scarce in the literature which is most likely why examples of topochemical controlled reactions of TTF derivatives are so few. Even so, the majority of [2+2] cyclisations of TTF derivatives do not proceed via a SCSC transformation. In the current study we report only the second SCSC reaction of a TTF derivative and the first example of a [2+2] photo-induced SCSC transformation for a co-facially stacked TTF derivative. In order to probe this hypothesis further, the synthesis of a range of TTF derivatives with electron-withdrawing substituents is currently in progress in our laboratory and X-ray crystallographic studies coupled with theoretical calculations are planned to further elucidate their reactivity in the solid state.

Notes and references

^a Department of Chemistry, Brock University, 500 Glenridge Ave, St. Catharines, ON, L2S 3A1, Canada. Tel.: +1 (905) 688 5550 Ext. 3403; E-mail: mpilkington@brocku.ca

^b Department of Chemistry, University of Cambridge, Lensfield Road, Cambridge, CB2 1EW, UK.

† Present address: Department of Chemistry and Biochemistry, University of Windsor, 401 Sunset Ave., Windsor, Ontario, Canada N9B 3P4.

† Electronic Supplementary Information (ESI) available: Detailed synthetic procedure for **1**; Tables of selected bond lengths and angles for **1-3**; DFT calculations for **1** and **3**. See DOI: 10.1039/b000000x/

- a) *Organic Solid State Reactions*, F. Toda (Ed.), *Top. Curr. Chem.*, 2005, **254**, Springer-Verlag; b) K. Tanaka and F. Toda, *Chem. Rev.*, 2000, **100**, 1025.
- N. J. Turro, V. Ramamurthy and J. C. Scaiano, *Modern Molecular Photochemistry of Organic Molecules*, University Science Books, 2010.
- a) M. D. Cohen and G. M. J. Schmidt, *J. Chem. Soc.*, 1964, 1996; b) M. D. Cohen, G. M. J. Schmidt and F. I. Sonntag, *J. Chem. Soc.*, 1964, 2000; c) G. M. J. Schmidt, *J. Chem. Soc.*, 1964, 2014; d) G. J. M. Schmidt, *Pure Appl. Chem.* 1971, **27**, 647.
- V. Ramamurthy and K. Venkatesan, *Chem. Rev.*, **1987**, *87*, 433.
- G. Kaupp, *Top. Curr. Chem.*, 2005, **254**, 95.
- A. G. Jarvis, H. A. Sparkes, S. E. Tallentire, L. E. Hatcher, M. R. Warren, P. R. Raithby, D. R. Allan, A. C. Whitwood, M. C. R. Cockett, S. B. Duckett, J. L. Clark and L. J. S. Fairlamb, *CrystEngComm*, 2012, **14**, 5564.
- a) *Molecular Crystals*, 2nd Edition, J. D. Wright, Cambridge University Press, 1995; b) F. H. Allen, M. F. Mahon, P. R. Raithby, G. P. Shields and H. A. Sparkes, *New J. Chem.*, 2005, **29**, 182.
- M. Nagarathinam, A. M. P. Peedikakkal and J. J. Vittal, *Chem. Commun.*, 2008, 5277.
- a) X. Gao, T. Friščić and L. R. MacGillivray, *Angew. Chem. Int. Ed.* 2003, **43**, 232; b) T. Friščić and L. R. MacGillivray, *Supramolecular Chemistry*, 2005, *17*, 47; c) L. R. MacGillivray, G. S. Papaefstathiou, T. Friščić, T. D. Hamilton, D.-K. Bucar, Q. Chu, D. B. Varshney and I. G. Georgiev, *Acc. Chem. Res.*, 2008, **41**, 280 and references therein.
- T. Caronna, R. Liantonio, T. A. Logothetis, P. Metrangolo, T. Pilati and G. Resnati, *J. Am. Chem. Soc.*, 2004, **126**, 4500.
- a) G. S. Papaefstathiou, Z. Zhong, L. Geng and L. R. MacGillivray, *J. Am. Chem. Soc.*, 2004, **126**, 9158; b) Q. Chu, D. C. Swenson and L. R. MacGillivray, *Angew. Chem., Int. Ed.*, 2005, **44**, 3569; c) N. L. Toh, M. Nagarathinam and J. J. Vittal, *Angew. Chem., Int. Ed.*, 2005, **44**, 2237; d) Y.-F. Han, Y.-J. Lin, W.-G. Jia, G.-L. Wang and G.-X. Jin, *Chem. Commun.*, 2008, 1807; e) M. Nagarathinam and J. J. Vittal, *Chem. Commun.*, 2008, 438–440; f) G. K. Kole, R. Medishetty, L. L. Koh and J. J. Vittal *Chem. Commun.*, 2013, **49**, 6298.
- a) N. I. Danilenko, M. I. Podgornaya, T. N. Gerasimova and E. P. Fokin, *Bull. Acad. Sci. USSR, Div. Chem. Soc.*, 1981, **30**, 1728; b) G. W. Coates, A. R. Dunn, L. M. Henling, J. W. Ziller, E. B. Lobkovsky and R. H. Grubbs, *J. Am. Chem. Soc.*, 1998, **120**, 3641.
- a) M. Mas Torrent and C. Rovira, *J. Mater. Chem.* 2006, **16**, 433; b) J. M. Williams, J. R. Ferraro, R. J. Thorn, K. D. Carlson, U. Geiser, H. H. Wang, A. M. Kini and M.-H. Whangbo, *Organic Superconductors (Including Fullerenes)*, *Synthesis, Structure, Properties and Theory*, Prentice Hall, 1992.
- Web of Knowledge search conducted 28/1/2014. For representative reviews, see: a) Y. Zheng and F. Wudl, *J. Mater. Chem. A*, 2014, **2**, 48; b) D. Canevet, M. Sallé, G. Zhang, D. Zhang and D. Zhu, *Chem. Commun.*, 2009, 2245; c) M. Bendikov, F. Wudl and D. F. Perepichka, *Chem. Rev.*, 2004, **104**, 4891; d) J. L. Segura and N. Martín, *Angew. Chem. Int. Ed.*, 2001, **40**, 1372; e) M. R. Bryce, *J. Mater. Chem.*, 1995, **5**, 1481.
- Y. N. Kreicberga, E. E. Liepins, I. B. Mazeika, and O. Y. Neilands, *Z. Org. Khim. (Engl. Trans.)*, 1986, **22**, 367.

- 16 P. Venugopalan and K. Venkatesan, *Bull. Chem. Soc. Jpn.*, 1990, **63**, 2368.
- 17 a) T. Devic, P. Batail and N. Avarvari, *Chem. Commun.*, 2004, 1538; b) T. Devic, P. Batail and N. Avarvari, *Chem. Eur. J.*, 2004, **10**, 3697.
- 18 O. Jeannin and M. Fourmigué, *Chem. Eur. J.*, 2006, **12**, 2994.
- 19 a) C. Simao, M. Mas-Torrent, V. André, M. T. Duarte, J. Veciana and C. Rovira, *Chem. Sci.*, 2013, **4**, 307; b) C. Simao, M. Mas-Torrent, V. André, M. T. Duarte, S. Techert, J. Veciana and C. Rovira, *Cryst.Eng.Comm.*, 2013, **15**, 9878.
- 20 T. Friščić and L. R. MacGillivray, *Z. Kristallogr.*, 2005, **220**, 351.
- 21 a) F. Leurquin, T. Ozturk, M. Pilkington and J. D. Wallis, *J. Chem. Soc., Perkin Trans. 1*, 1997, 3173; b) T. Ozturk, N. Saygili, S. Ozkara, M. Pilkington, C. R. Rice, D. A. Tranter, F. Turksy and J. D. Wallis, *J. Chem. Soc., Perkin Trans. 1*, 2001, 407; c) N. Saygili, R. J. Brown, P. Day, R. Hoelzl, P. Kathirgamanathan, E. R. Mageean, T. Ozturk, M. Pilkington, M. M. B. Qayyum, S. S. Turner, L. Vorwerg and J. D. Wallis, *Tetrahedron*, 2001, **57**, 5015; d) S.-X. Liu, A. Neels, H. Stoeckli-Evans, M. Pilkington, J. D. Wallis and S. Decurtins, *Polyhedron*, 2004, **23**, 1185.
- 22 a) S.-X. Liu, S. Dolder, M. Pilkington and S. Decurtins, *J. Org. Chem.*, 2002, **67**, 3160; b) M. Chahma, X. Wang, A. van der Est, and M. Pilkington, *J. Org. Chem.*, 2006, **71**, 2750; c) M. Chahma, N. Hassan, A. Alberola, H. Stoeckli-Evans and M. Pilkington, *Inorg. Chem.*, 2007, **46**, 3807.
- 23 a) M. Chahma, K. Macnamara, A. van der Est, A. Alberola, V. Polo and M. Pilkington, *New J. Chem.*, 2007, **31**, 1973; b) A. Alberola and M. Pilkington, *Current Organic Synthesis*, 2009, **6**, 66.
- 24 a) R. T. Boeré, R. T. Oakley and R. W. Reed, *J. Organometal. Chem.*, 1987, **331**, 161; b) P. Del Bel Belluz, A. W. Cordes, E. M. Kristof, P. V. Kristof, S. W. Liblong and R. T. Oakley, *J. Am. Chem. Soc.*, 1989, **111**, 9276; c) J. M. Rawson, A. J. Banister and I. Lavender, *Adv. Het. Chem.*, 1995, **62**, 137; d) C. M. Aherne, A. J. Banister, I. B. Gorrell, M. I. Hansford, Z. V. Hauptman, A. W. Luke and J. M. Rawson, *J. Chem. Soc., Dalton Trans.*, 1993, 967; e) J. M. Rawson and J. J. Hayward, *Handbook of Chalcogen Chemistry: New Perspectives in Sulfur, Selenium and Tellurium 2*, 2013, **2**, 69.
- 25 a) G. R. Desiraju and R. L. Harlow, *J. Am. Chem. Soc.*, 1989, **111**, 6757; b) P. Metrangolo, H. Neukirch, T. Pilati and G. Resnati, *Acc. Chem. Res.*, 2005, **38**, 386; c) A. D. Bond, J. Griffiths, J. M. Rawson and J. Hulliger, *Chem. Commun.*, 2001, 2488.
- 26 a) D. A. Haynes, *CrystEngComm*, 2011, **13**, 4793; b) A. W. Cordes, R. C. Haddon, R. G. Hicks, R. T. Oakley and T. T. M. Palstra, *Inorg. Chem.*, 1992, **31**, 1802; c) A. Alberola, R. J. Less, F. Palacio, C. M. Pask and J. M. Rawson, *Molecules*, 2004, **9**, 771; d) M. Fourmigué and P. Batail, *Chem. Rev.* 2004, **104**, 5379.
- 27 a) C. R. Ojala, W. H. Ojala and D. Britton, *J. Chem. Crystallogr.*, 2011, **41**, 464; b) G. R. Desiraju, *Angew. Chem. Int. Ed. Engl.*, 1995, **34**, 2311; c) G. R. Desiraju and T. Steiner, *The Weak Hydrogen Bond in Structural Chemistry and Biology*, Oxford University Press, Oxford, 1999.
- 28 M. Iyoda, Y. Kuwatani, N. Uenob and M. Odab, *Chem. Commun.*, **1992**, 158.
- 29 R. Ditchfield, W. J. Hehre, and J. A. Pople, *J. Chem. Phys.*, 1971, **54**, 724.
- 30 C. Lee, W. Yang and R. G. Parr, *Phys. Rev. B*, 1988, **37**, 785.
- 31 Jaguar version 8.0, Schrödinger LLC, New York, NY, 2013.
- 32 V. Polo, A. Alberola, J. Andres, J. Anthony and M. Pilkington, *Phys. Chem. Chem. Phys.*, 2008, **10**, 857.
- 33 R. W. W. Hoof, *COLLECT*. Nonius BV, Delft, The Netherlands, 1998.
- 34 Z. Otwinowski. and W. Minor, *Methods in Enzymology*, Vol. 276, *Macromolecular Crystallography*, Part A, C. W. Carter, Jr. and R. M. Sweet (eds.), pp. 307-326. New York: Academic Press, 1997.
- 35 R. H. Blessing, *Acta Cryst.*, 1995, **A51**, 33.
- 36 Bruker 2012, AXS Inc., Madison, Wisconsin USA
- 37 G. M. Sheldrick, *Acta Cryst.*, 2008, **A64**, 112.
- 38 A. L. Spek, *Acta Cryst.*, 2009, **D65**, 148.
- 39 J. Sun, X. Lu, J. Shao, X. Li, S. Zhang, B. Wang, J. Zhao, Y. Shao, R. Fang, Z. Wang, W. Yu and X. Shao, *Chem. Eur. J.*, 2013, **19**, 12517.
- 40 K. Gnanaguru, N. Ramasubbu, K. Venkatesan and V. Ramamurthy, *J. Org. Chem.*, 1985, **50**, 2337.

Probing the unusual single crystal-to-single crystal [2+2] photocyclization reaction of a TTF-aryl-nitrile derivative.

John J. Hayward, Roger Gumbau-Brisa, Antonio Alberola, Caroline S. Clarke, Jeremy M. Rawson and Melanie Pilkington

Irradiation of single crystals of a benzonitrile substituted tetrathiafulvalene with polychromatic light results in a [2+2] cycloaddition reaction. In contrast, the pyridyl derivative shows no such photoreactivity under the same conditions.

